Challenges and Solutions in the Development of a Johnson Noise Thermometer

Paul Bramley[1, a)] and David Cruickshank[1, b)]

[1]*Metrosol Ltd, Plum Park Estate, Watling Street, Paulerspury, Northamptonshire, NN12 6LQ, UK*

[a)]Corresponding author: paul.bramley@metrosol.co.uk
[b)]david.cruickshank@metrosol.co.uk

Abstract. Johnson noise thermometers are of interest for two main reasons. Firstly, with the redefinition of the Kelvin in 2019 [1], [2] there is a need for a practical primary thermometer that makes use of the newly fixed Boltzmann constant to realize the Kelvin [3]. Secondly, a Johnson noise thermometer measures all the properties required to determine true thermodynamic temperature and as such is immune to the problem of calibration drift due to changes in the sensor that all current practical thermometers experience and which is a particular problem in harsh environments. We have developed a new technique for the realization of a practical Johnson noise thermometer that overcomes the problems with prior art realizations and offers adequate uncertainty within a response time that is acceptable for metrology and industrial applications (0.1 % in 5.3 s) [4], [5]. In trying to realize a practical implementation of this technique, we have encountered several technical problems. These include the difficulty in generating a calibration signal with low uncertainty (<0.01 %) over the working bandwidth 10 kHz - 1 MHz, minimizing aberrations that contaminate the calibration signal and the effect of electrical conduction in the probe insulation at high temperature. We also briefly discuss improving the signal processing delay so that temperature measurements can be made in real time.

INTRODUCTION

All thermometers currently used in temperature metrology and industrial temperature measurement are prone to drift, which leads to increasing and sometimes unacceptable uncertainty in the measurements made. They drift because thermometers such as thermocouples or resistance temperature detectors (RTDs) are secondary thermometers. They do not measure temperature directly, instead they measure a property of the sensor that varies with temperature. Provided the relationship between temperature and the property is known (its calibration), the temperature can be inferred by measuring the property. However, factors other than temperature can affect the measured property, leading to a change in the calibration of the sensor and consequently a drift in the indicated temperature. This is a particular problem if low uncertainty is required (metrology applications) and in harsh environments (e.g. high temperature, high shock/vibration, contaminating or nuclear environments).

A solution is to use a primary thermometry technique, which exploits a fundamental physical law involving temperature. By solving the associated equation for temperature and measuring the required variables simultaneously in real time, it is possible to determine true thermodynamic temperature thereby providing drift-free temperature measurement. There is also a need from metrologists for primary thermometers following the redefinition of the Kelvin [1], [2]. There are a few primary thermometer types in development [3], one of which is Johnson noise thermometry (JNT).

Johnson noise (also known as thermal noise or Johnson-Nyquist noise) was first observed by John Johnson at Bell labs in 1927 [6] and explained by Harry Nyquist in 1928 [7]. It is generated by the thermally excited random motion of the carriers in a conductive medium. Since the electrons have a discrete, quantized charge their random motion leads to a small alternating current (AC) signal appearing across the conductive material because they are not equally distributed across the conductor at any instant in time. In effect, the charge on the electrons allows their average kinetic energy (their thermodynamic temperature) to be measured by measuring the electrical noise they create. The Johnson

noise across a conductor is therefore directly related to the temperature of the electrons in the conductor. The Johnson-Nyquist equation can be used to determine temperature as shown in equation 1:

$$T = \frac{1}{4k}\left\{\frac{V_n^2}{R\Delta f}\right\} \quad (1)$$

Where T is the thermodynamic temperature, k is the Boltzmann constant (defined as 1.380649×10^{-23} JK^{-1} by international agreement in 2019 [1]), V_n is the root mean square (RMS) Johnson noise, R is the resistance of the sensor and Δf is the bandwidth of the measurement system.

PRIOR ART NOISE THERMOMETERS USING TIME DOMAIN SIGNAL SEPARATION

Many attempts to realize a thermometer based on the measurement of Johnson noise have been made since as far back as the late 1950s [8], [9], but there are still not any commercially available thermometers based on Johnson noise. In large part this is due to the difficulty of measuring the extremely small Johnson noise signals with sufficient precision. It has also proved difficult to make the measurement sufficiently immune to external electromagnetic interference because of the very small signals involved. Like many measurements, Johnson noise is usually measured by making a ratio comparison between the unknown Johnson noise and a reference signal that has a known power spectral density. Prior art systems typically make the comparison by switching the measurement system between measuring the unknown Johnson noise and a reference signal (time-domain signal separation) [8], [9]. However, as the system switches between the two measurements, there is a change in the measurement bandwidth that leads to potentially very significant measurement uncertainty. The only effective mitigation was to limit the measurement bandwidth to well below that caused by the sensor's resistor-capacitor (*RC)* time constant.

There is a fundamental uncertainty associated with Johnson noise thermometry due to the nature of random processes as defined by Rice's equation [10], which states that the fractional standard deviation of the measured noise signal is:

$$\frac{\sigma_{V_n}}{V_n} = \frac{1}{\sqrt{\Delta f \Delta t}} \quad (2)$$

Where: σ_{V_n} is the standard deviation of the Johnson noise root mean square (RMS) voltage V_n in bandwidth Δf measured in a time interval of Δt. Limiting the measurement bandwidth means that long measurement times are required to achieve the required uncertainty. From equations (1) and (2), the fractional standard deviation of the indicated temperature is:

$$\frac{\sigma_T}{T} = \frac{2}{\sqrt{\Delta f \Delta t}} \quad (3)$$

Note that equation (3) only applies to a single measurement and is applicable to the proposed system. Prior art systems typically switch between measuring the sensor signal and a reference signal and will usually take twice as long (or Δt is half of the available measurement time). This increases the fractional standard deviation in a given time by a factor of $\sqrt{2}$. Accordingly, a typical (prior art system) using 100 kHz bandwidth requires ~8.9 hours to achieve 0.01 % uncertainty with 95 % confidence, equivalent to 0.030 K at 25° C and 0.13 K at 1,000 °C. These calculations only consider uncertainty caused by the random process being measured, there will be other sources of uncertainty in practical systems such as amplifier noise. If the practical system uncertainty is close to the Rice's equation uncertainty, then the practical implementation is as good as can be achieved without changing the parameters in Rice's equation.

PROPOSED SYSTEM

The authors have devised a system (see Fig. 1) for separating the Johnson noise from a reference signal in the frequency domain [4], [5] that overcomes the bandwidth change problem when switching between a sensor and a reference. They have also developed a realization that overcomes the problem of electromagnetic immunity allowing

the JNT to operate in electrically noisy, real-world environments by employing a full coaxial design [11], [12]. Some details regarding the operation of the system are given in prior publications [4], [5].

The proposed system also uses many techniques previously proposed for JNT [8], [9], [13]. These include calibration tones to form a Pseudo Random Noise (PRN) reference signal, this replaces a known resistor at a known temperature in many earlier systems. It uses synchronous sampling between the generation of the calibration tones and the received signal sampling which allows the calibration tones to be confined to individual and known bins in the Fast Fourier Transform (FFT) after the sampling. Correlation is done in the frequency domain as this is more computationally efficient than time domain processing [14]. The new approach injects the PRN signal as a current rather than switching to a voltage calibration signal and thereby allows two of the variables in equation 1 to be measured. The measurement of the voltage generated allows the resistance to be determined from Ohm's law (as a function of frequency). The PRN signal is a series of impulse functions in the frequency domain, so samples the frequency response of the system and allows the measurement bandwidth to be determined.

Each of the two amplifiers has multiple stages to allow high gain and maintain bandwidth throughout. The first stage of the amplifier needs to have low voltage and current noise and high input impedance. This means the proposed system and most other JNT system amplifiers have a Junction Field Effect Transistor (JFET) based first stage [15]. The other gain stages of the amplifier in the proposed system are operational amplifier based. The resistors that define the gain of these amplifiers are high precision (0.01 % initial tolerance) and have low temperature coefficient of resistance (TCR), 2 $ppmK^{-1}$.

The anti-aliasing filters are currently simple low order analogue filters. The amplified signals are then digitized by two 24 bit analogue to digital converters (ADCs) [16], [17] with initial sampling at 20 million samples per second, 20 MSs^{-1}. The digitized signal is then filtered using a 96-tap finite impulse response (FIR) filter with a cut off frequency of 1 MHz and a stop band rejection of 120 dB at 1.25 MHz. This allows the signal to be decimated by a factor of 8, giving a new sample rate of 2.5 MS/s.

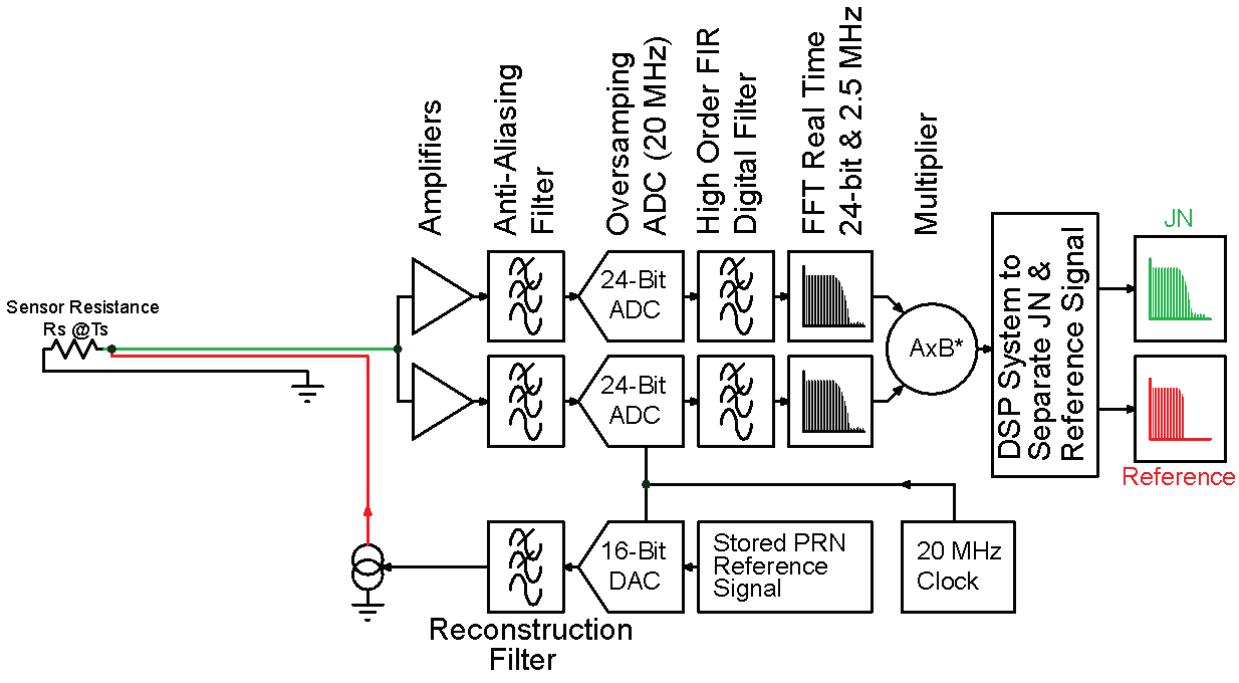

FIGURE 1. Johnson Noise Thermometer Using Frequency Domain Signal Separation

The outputs of the two ADCs are then sent to a personal computer (PC) for further signal processing. The PC implements correlation in the frequency domain by taking the two ADC outputs, performing a $2^{17} = 131072$-point FFT on each and multiplying one by the complex conjugate of the other to give a cross-correlation spectrum. Cross-correlation in the frequency domain is more computationally efficient than cross-correlation in the time domain [14].

This correlation technique is a standard way for reducing amplifier noise in JNT systems [13]. To further reduce noise, 100 cross-correlation spectra are accumulated. This gives a PRN waveform time of 131072 / 2500000 = 0.0524 s and a measurement time of (100×131072) / 2500000 = 5.243 s.

Prior art systems have used a known resistor at a known temperature to provide a reference signal to calibrate JNTs and determine thermodynamic temperature [8]. Another approach is to use a synthetic signal to provide a reference. Very low uncertainty can be obtained from a JNT using a quantum-accurate voltage-noise source (QVNS) to create the PRN signal [9], [13]. However, such a system requires cryogenic cooling and is therefore not practical for many applications. In most prior systems, the sensor and the calibration signal are time multiplexed, the circuitry switches from one to the other [9]. Any system that switches the input from the sensor to a reference source has the problem of changes in bandwidth between the sensor and the calibration signal which can lead to error in the measured temperature.

The proposed system uses a calibration signal superimposed on the Johnson noise to provide system calibration without switching. This signal comprises a series of harmonically related ("comb of") sinusoidal tones with randomized phase that form a PRN signal in the time domain. These tones are arranged to be exclusively in one FFT bin at the end of the signal processing, avoiding spectral leakage [13] and allowing them to be separated from the Johnson noise. Stored samples of the calibration waveform are turned into an analogue signal by streaming them from memory to a digital to analogue converter (DAC) [17]. To keep each tone exclusively within one FFT bin at the end of the signal processing, the DAC clock must be derived from the same clock as the ADC [16]. The simplest arrangement is to make the DAC and the ADC sample clock the same, as shown in Fig. 1, but there are advantages in using a multi-rate system where the DAC and the ADC operate at different sample rates, see below. However, to continue to avoid spectral leakage, any sine wave in the DAC signal must continue to have a period that is an integer fraction of the waveform time, and the DAC sampling clock must have an exact known relationship with the ADC clock. In practice this means the ADC and DAC clock are derived from the same oscillator.

In the proposed system, the calibration signal output is injected into the system as a current. The DAC output signal is attenuated to avoid saturating the amplifiers and then injected into the measurement system via a high value resistor, approximating a current source.

The sine waves (tones) from the calibration signal can be selected from the output signal since their frequencies and bin numbers are pre-determined from the choice of calibration signal. There is of course Johnson Noise in the same bin, the calibration signal may be sufficiently large in comparison for the Johnson noise in the same bin to be ignored or an estimate of the Johnson noise can be subtracted from the calibration signal. This subtraction needs to be done as a mean square subtraction since the Johnson noise is random, zero mean and uncorrelated with the calibration signal. The practical realization of the system employed a full coaxial design [11], [12] to overcome the problem of electromagnetic immunity, allowing the JNT to operate in electrically noisy, real-world environments. Some details regarding the operation of the system are given in prior publications [4], [5].

A segment of the continuous PRN used is shown in Fig. 2 together with the stepped realization (zero-order hold filter function) [16] version generated by the digital to analogue converter (DAC). Figure 3 shows the power distribution of the stepped PRN signal in the frequency domain, together with an ideal "brick wall" reconstruction filter (which cannot be realized in practice) to remove these unwanted images and a 5-pole low-pass filter as an example of a realizable reconstruction filter.

The effect of the stepped realization (Zero-Order Hold Function) is to create images of the continuous PRN signal in the frequency domain at integer multiples of the sample frequency that are amplitude modulated by a sinc^2 function [16]:

$$H_P(f) = \left[sinc\left(\pi \frac{f}{f_s}\right)\right]^2 = \left[\frac{f_s}{\pi f}\sin\left(\pi \frac{f}{f_s}\right)\right]^2 \tag{4}$$

where $H_p(f)$ is the scaling factor (power) at frequency f in a system using a sample frequency of f_s.

This means that the first image at 20 MHz would be aliased down to DC and span -1 MHz to +1 MHz when resampled at a frequency of 20 MHz by the analogue to digital converter (ADC). The images are attenuated (but not eliminated) by analog, low-pass filters in the system, but the components in the filters have a tolerance and change with time and temperature, leading to measurement uncertainties. The filter's corner frequency needs to be kept significantly above the PRN signal's spectrum to minimize the propagation of uncertainty in the value of the analog components into the passband frequency response. The corner frequency also needs to be kept as low as possible to attenuate the PRN images adequately and mitigate the uncertainty arising from aliasing into the PRN's spectrum. These two design constraints contradict each other.

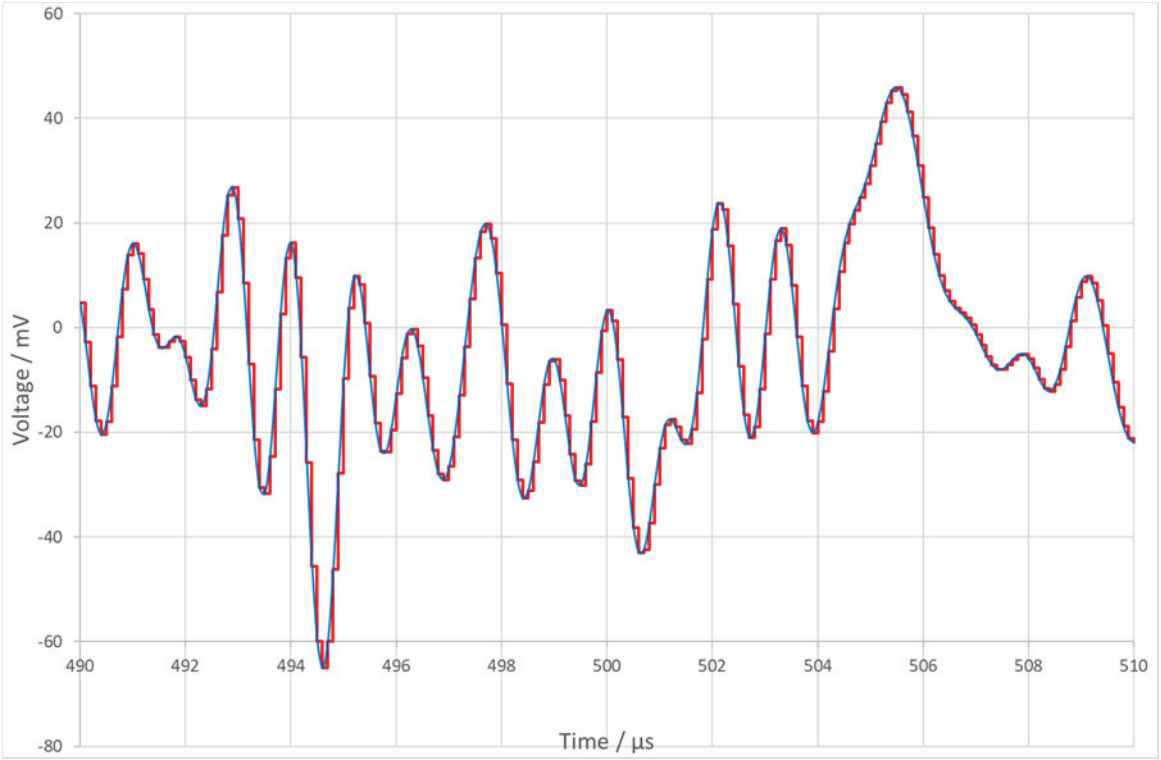

FIGURE 2. PRN Signal and Zero-Order Hold Function Realization [16] (Time Domain)

A multi-rate system [20] was devised in which the ADC and DAC operate at different frequencies, which reduces the aliasing problem by orders of magnitude. By generating the PRN with the DAC at a sample frequency of 22 MHz and resampling the signal at a frequency of 20 MHz with the ADC, the first image (at 22 MHz) is aliased down to a center frequency of 2 MHz, so it spans 1 to 3 MHz, thereby missing the PRN spectrum as shown in Fig. 4:

The Effect of Imperfections of DACs Used to Generate Reference Signals

The first full system design used an R-2R DAC to create the PRN signal. Details of this DAC architecture can be found in [17]. However, when we viewed the spectrum of the PRN after resampling with the ADC and processing with the FFT, we noticed that whilst the tones peaks were clearly visible, there were a lot of spurious signals in the gaps where we expected no signal (see Fig. 5). Various methods were employed to investigate this problem until we eventually removed the expected tones from the spectrum and then applied an inverse FFT to view the error signal in the time domain. We then noticed spikes (glitches) at specific voltage transitions in the waveform. This is the problem of glitch impulse energy that is a characteristic of DACs, the voltage spikes that occur as a DAC output changes from one value to another [18], [19].

The solution was to use a current steering DAC. These have glitch impulse energies that are several orders of magnitude smaller than their R-2R counterparts. No spurious signals were visible and the contrast between the peaks and any signal in the gaps (now just unstructured noise) increased from a barely adequate ~$10^{4.5}$ for the R-2R DAC (Fig. 5) to >10^{7} for the current steering DAC (Fig. 6):

The Contribution of Insulation Leakage to Measurement Uncertainty

It is important that the Johnson noise measured is from the sensor resistance and nowhere else. We use a 4-wire connection to the sensor element, with the two coaxial connections going to the two correlator inputs. This means that the correlator suppresses any Johnson noise that occurs in the connecting leads, giving a noise measurement of the

signal at the point where the connection pairs meet (at the sensor). This is analogous to the 4-wire connections used to eliminate the effect of lead resistance in precision resistance measurements.

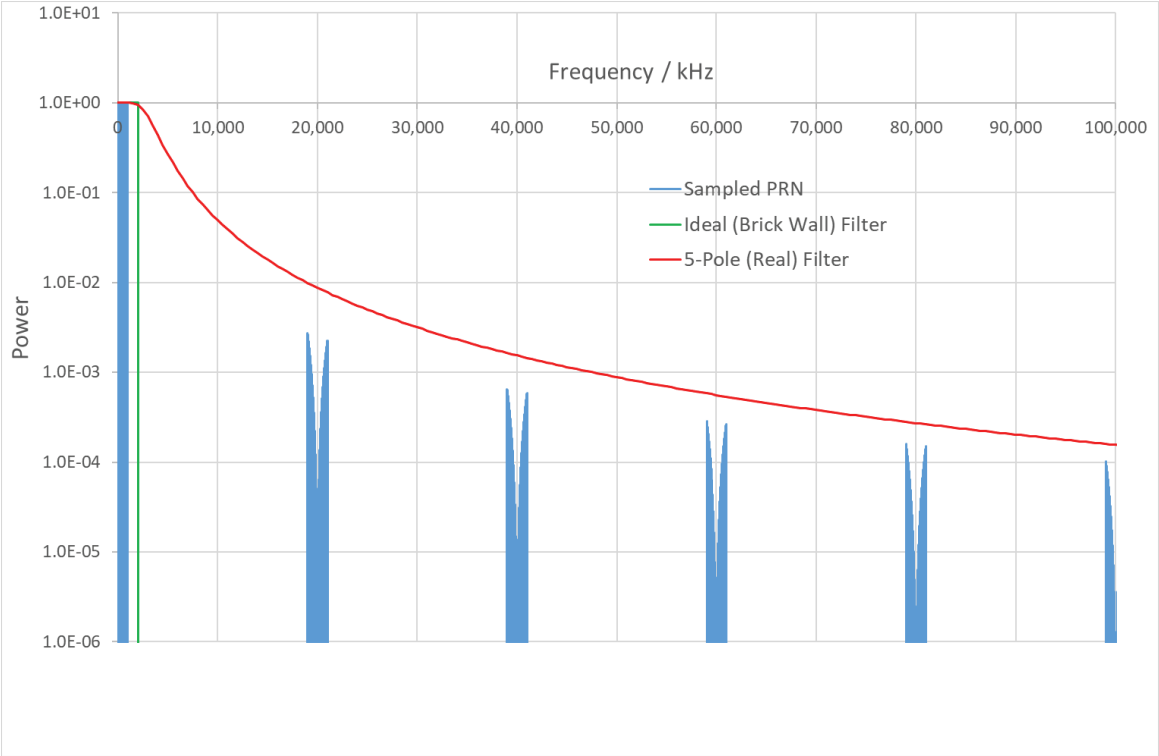

FIGURE 3. Zero-Order Hold Function Realization of PRN Signal and Image Suppression Filters. Sample frequency, fs, is 20 MHz

Another source of Johnson noise generated in the thermometer probe also needs to be considered. At high temperatures, the electrical insulation in the probe will start to conduct. In our work so far, this is a resistive (dissipative) medium so will generate Johnson noise that has not come from the sensor element and its effect needs to be considered. The insulation would typically be a ceramic such as alumina, although there are better ceramic materials and glasses than alumina for this kind of application. As well as the changes in conductivity at high temperatures, in some materials, there will be changes in dielectric properties at high temperature [21] which will create frequency dependent changes [22]. For simplicity, we can model the effect of leakage as a pure resistive problem, the extension to a frequency dependent impedance is possible. We model the leakage effect by considering two resistors at two different temperatures as shown in Fig. 7. We can calculate the effective resistance and Johnson noise appearing across them in Eq. 5:

$$R = \frac{R_1 R_2}{R_1 + R_2} \tag{5}$$

$$V_n = \sqrt{4k\Delta f \frac{T_1 R_1 R_2^2 + T_2 R_2 R_1^2}{(R_1 + R_2)^2}} \tag{6}$$

If we now put equations 5 & 6 back into equation 1, we see that the indicated temperature would be given by equation 7.

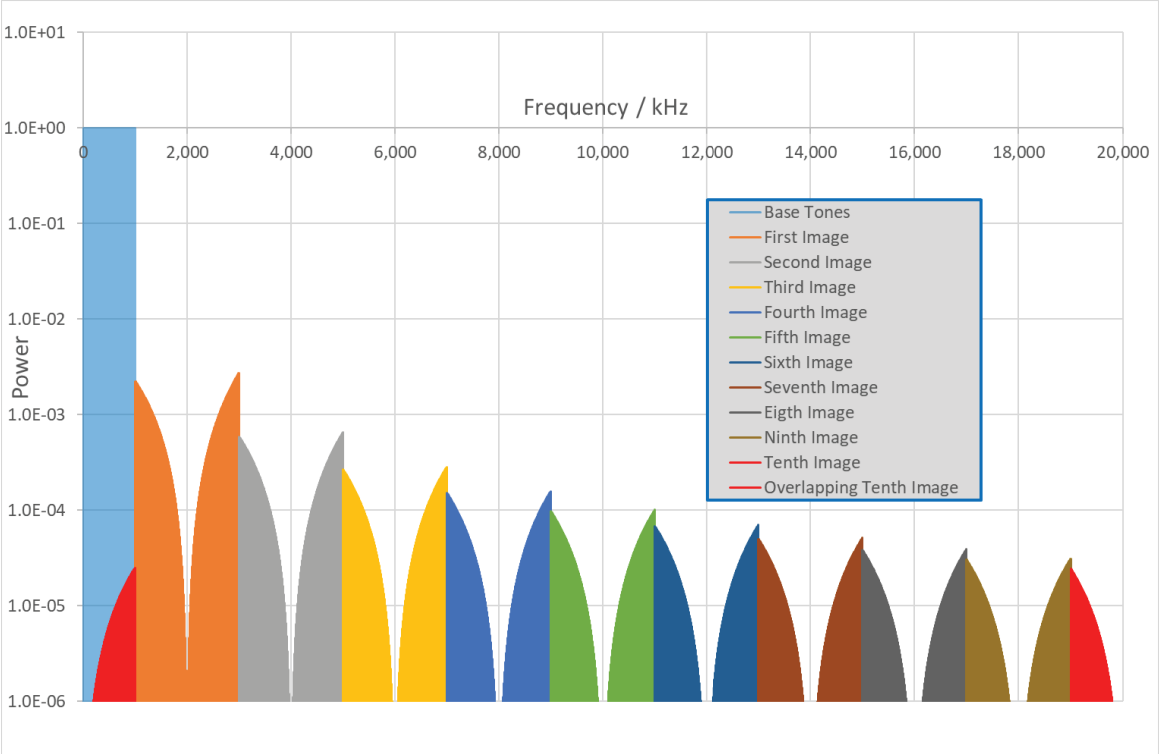

FIGURE 4. Spectrum of Multi-Rate PRN System

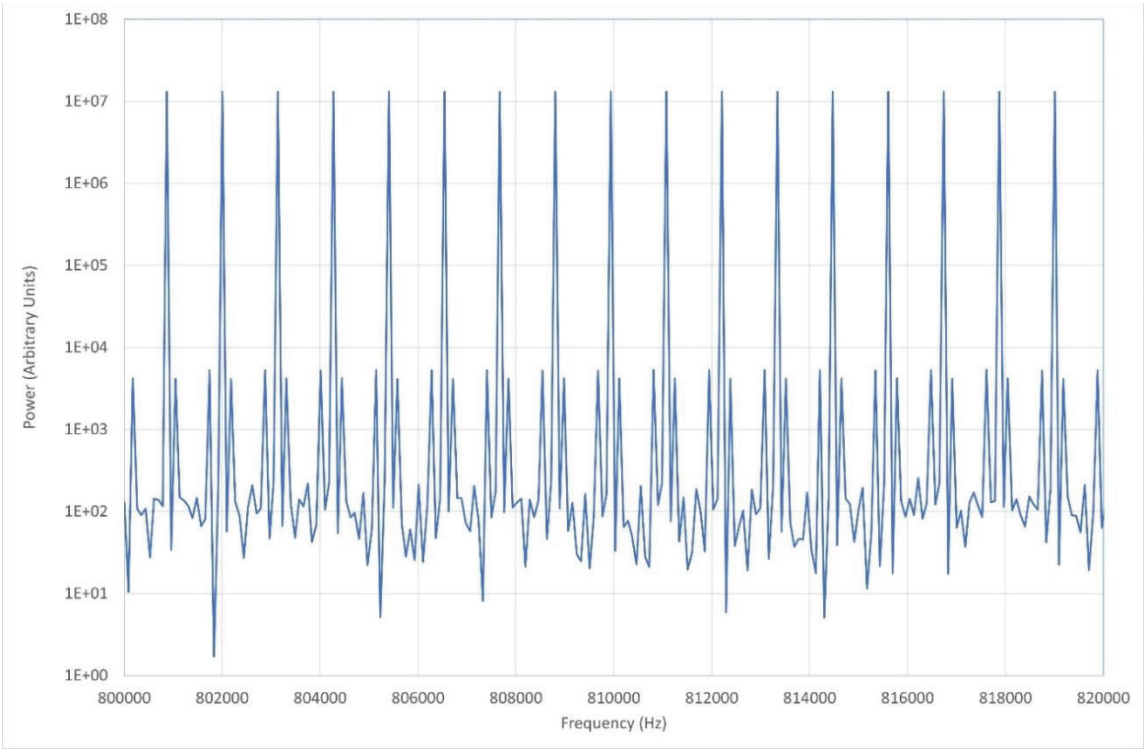

FIGURE 5. Spectrum of PRN Signal From R-2R DAC. The desired tones are the signals with power above 1.00E7 spaced by 1220 Hz. The signals in between these tones are the result of DAC glitch impulse energy

$$T = \frac{R_2 T_1 + R_1 T_2}{R_1 + R_2} \tag{7}$$

The insulation conduction has no effect if the resistors are at the same temperature ($T1 = T2 = T$). It also has no effect if the conduction is sufficiently low ($R2 \to \infty \Rightarrow T = T1$).

The implications for the probe design are shown in Fig. 8.

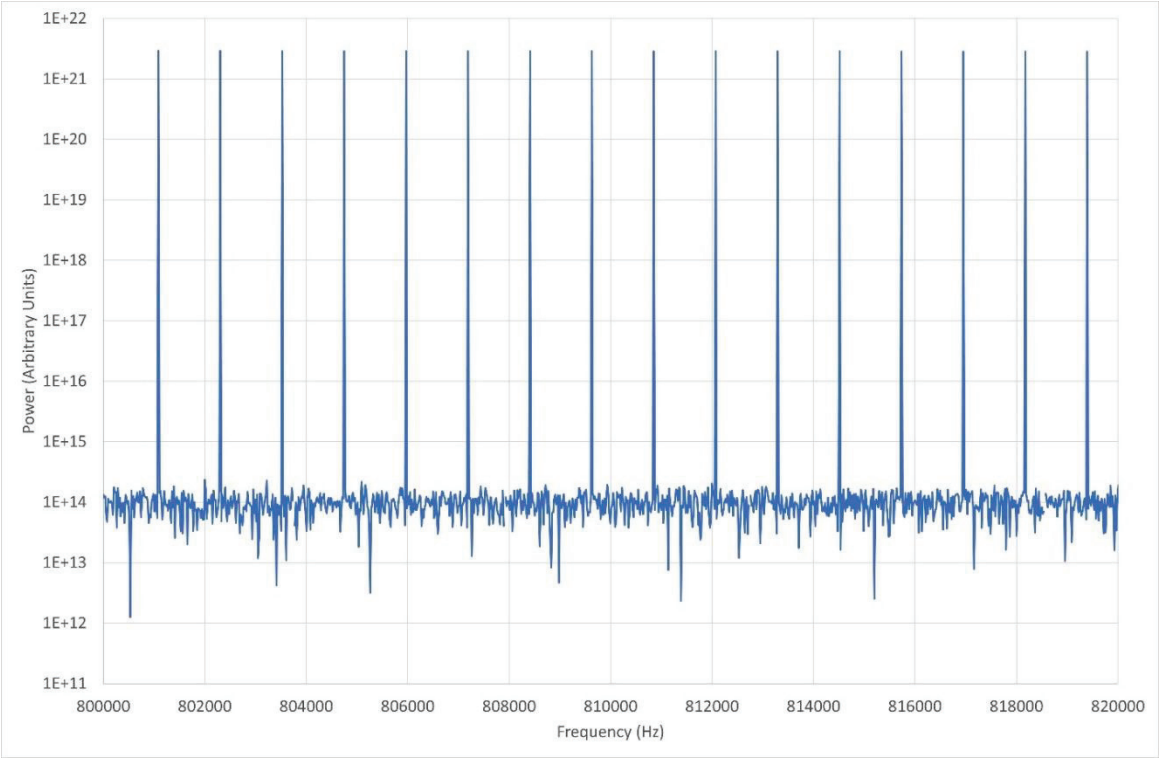

FIGURE 6. Spectrum of PRN Signal from Current Steering DAC

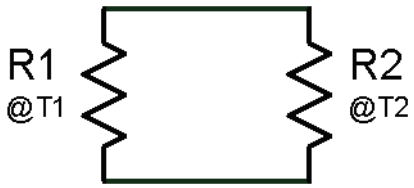

FIGURE 7. Effect of Insulation Leakage in Probe

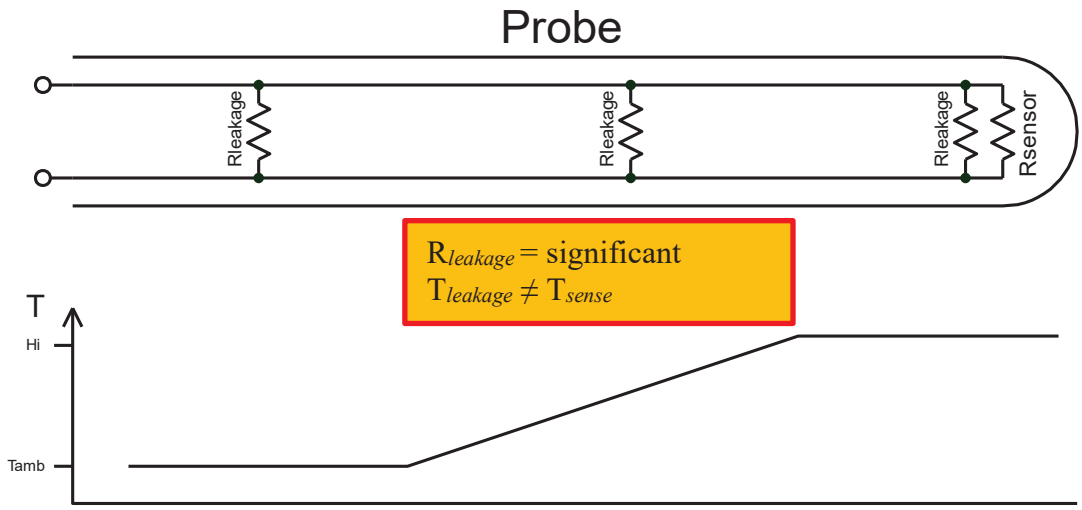

FIGURE 8. Effect of Insulation Leakage Resistance on Indicated Temperature

Any conduction near to the sensor element has no effect as it is at the same temperature as the sensor element. The insulation conductance at the cold end of the probe is sufficiently low to have no effect. However, there is a transition zone where the insulation conductance could be significant whilst also being at a different temperature from the sensor, leading to an error in the indicated value. The only mitigation is to ensure that the insulator used does not conduct significantly in comparison with the sensor at the maximum operating temperature. This is challenging since our system uses a 5 kΩ sense resistance to optimize other properties.

Real Time Signal Processing

The signal processing involves processing incoming 24-bit data at 2.5 MHz (decimated down from 20 MHz after the FIR digital filter realized in hardware) on two channels, converting these to the frequency domain using a 2^{17} length FFT and then accumulating 100 spectra to generate an accumulated spectrum every 5.243 s. This is then processed to determine the variables in equation 1 and therefore determine temperature. This process represents a significant processing demand. Initially this was done using a high-performance personal computer (PC) with a liquid cooled, state-of-the-art processor. Even with this processing power, the software took several minutes to process each 5.243 s accumulated spectrum.

We have now improved the software so that it can process accumulated spectra in less than the data acquisition time thereby making real-time measurement possible (with a processing latency). This was achieved on the same hardware as before by making 2 changes:

1. Manually dividing up the processing between the processor cores in the software (operating systems do not do this).
2. Installing the Intel Integrated Performance Primitives. "The Intel® Integrated Performance Primitives (Intel® IPP) is a software library that provides a comprehensive set of application domain-specific highly optimized functions for signal, data, and image processing." This library includes FFT functions highly optimized for execution speed.

CONCLUSIONS

We have presented some significant progress in key technologies required for JNT. We have examined the limitations imposed by Rice's equation which gives a theoretical best performance for JNT systems. We have proposed a multi-rate signal processing system that greatly reduces the required performance of the analogue anti-aliasing filter required in front of the ADC. We have discussed the degradation in performance that would occur if a DAC with high glitch energy was used to generate reference signals and proposed and tested a better system. We have discussed the issue of the electrical insulators in a probe starting to conduct at high temperatures and developed

models for this effect. We have also discussed techniques to speed up the considerable signal processing required to process the data from a JNT system so temperatures can be obtained in real time.

REFERENCES

1. B. Fellmuth, J. Fischer, G. Machin, S. Picard, P. P. M. Steur, O. Tamura, D. R. White and H. Yoon, Phil. Trans. R. Soc. A **374**, (2016).
2. G. Machin, M. Sadli, J. Pearce, J. Engert and R. M. Gavioso, Measurement **201**, (2022).
3. S. Dedyulin, Zeeshan Ahmed and G. Machin, Meas. Sci. Technol. **33**, (2022).
4. P. Bramley, D. Cruickshank, J. Aubrey, Meas. Sci. Technol. **31**, (2020).
5. P. Bramley, D. Cruickshank, J. Pearce, Int. J. Thermophys. **38**, (2017).
6. J. B. Johnson, Nature **119**, 50-51 (1927).
7. H. Nyquist, Phys. Rev. **32**, 110-113 (1928).
8. D. R. White, R. Galleano, A. Actis, H. Brixy, M. De Groot, J. Dubbeldam, A. L. Reesink, F. Edler, H. Sakurai, R. L. Shepard, and J. C. Gallop, Metrologia **33**, (2003).
9. J. F. Qu, S. P. Benz, H. Rogalla, W. L. Tew, D. R. White, K. L. Zhou, Meas. Sci. Technol., 30, 11, (2019).
10. S. O. Rice, Bell Syst. Tech. J. **23**, 282-332 (1945).
11. B. Kibble, G. Rayner, *Coaxial AC Bridges*, (CRC Press, Bristol, 1984).
12. S. Awan, B. Kibble, J. Schurr, *Coaxial Electrical Circuits for Interferene-Free Measurements*, (Institution of Engineering and Technology, London, 2011).
13. N. E. Flowers-Jacobs, A. Pollarolo, K. J.Coakley, A. C. Weis, A. E. Fox, H. Rogalla, W. L. Tew, S. P. Benz, J. Res. Natl. Inst. Stand. Technol. **122**, (2017).
14. Dickman, *Verified Signal Processing Algorithms in MATLAB and C* (Springer Nature, Cham, 2022).
15. D. R. White, E. Zimmermann, Metrologia **37**, (2003).
16. M. J. M. Pelgrom, *Analogue-To-Digital Conversion*, (Springer Nature, Cham, 2022).
17. W. Kester (Editor) *The Data Conversion Handbook*, (Newnes, Burlington, 2005).
18. J. D. Lenk, *Simplified Design of Data Converters*, (Newnes, Newton, 1997).
19. How To Perform Accurate Measurement and Reduction of Glitch Impulse Energy in DACs, (Analog Devices Technical Articles, 2021).
20. F. J. Harris*, Multirate Signal Processing for Communication Systems*, (River Publishers, Gistrup, 2021).
21. L. Y. Chen, "Dielectric performance of a high purity HTCC alumina at high temperatures: A comparison study with other polycrystalline alumina", in Proceedings of International Conference and Exhibition on High Temperature Electronics, (2014), pp. 271-277.
22. K. Yamazawa, W. L. Tew, A. Pollarolo, H. Rogalla; P. D. Dresselhaus, S. P. Benz "Improvements to the Johnson noise thermometry system for measurements at 505 -800 K", in Temperature: Its Measurement and Control in Science and Industry - 2012, AIP Conf. Proc. 1552, edited by C. W. Meyer, (American Institute of Physics, Los Angeles, California, 2013), pp. 50–55.55.